Incommensurate Structure of a Lillianite-Type Samarium Chromium Sulfide Sm$_{2/3}$Cr$_2$S$_4$

A. Lafond,[1] L. Cario, A. van der Lee,* and A. Meerschaut

*Institut des Matériaux de Nantes, UMR-CNRS 110, Laboratoire de chimie des solides, 2, rue de la Houssinière, 44072 Nantes Cedex 02, France; and *LMPM, 8, rue de l'Ecole Nornale, 34053 Montpellier Cedex 01, France*

The structure of Sm$_{2/3}$Cr$_2$S$_4$ has been solved from single-crystal X-ray diffraction data. This compound presents a $3 \times a$ superstructure along **a** and an incommensurate superstructure along **b** close to $3 \times b$. The basic structure is described in the space group *Pmnb* with $a = 3.5030(3)$ Å, $b = 10.9199(8)$ Å, $c = 12.7987(8)$ Å, $Z = 4$, $R = 0.046$ for 916 observed reflections. The modulated structure refinement, taking into account the two superstructures, was carried out in a $(3 + 2)$D superspace group and leads to $R = 0.063$ for 1706 reflections. This structure consists of staggered double columns of [CrS$_6$] octahedra connected by samarium atoms in a trigonal prismatic bicapped environment. This structure is reminiscent of that found in the lillianite mineral family. The statistical occupancy of samarium atoms (1/3), in agreement with the charge equilibrium (Sm^{3+}, Cr^{3+}, S^{2-}), is related to the superstructure.   © 1996 Academic Press

INTRODUCTION

The existence of *Ln*Cr$_3$S$_6$ phases in the *Ln*–Cr–S system is already known (1). The structure of the Gd derivative was recently determined (2). A tripled superstructure along the **a** direction which is related to an atomic distribution on the Gd sites is reflected by a reformulation of the composition to Gd$_{2/3}$Cr$_2$S$_4$. This kind of structure is reminiscent of the arrangements found in the lillianite mineral family (3,4). Such a structure is generally adopted for some AB_2O_4 compounds with a large A^{2+} cation. As samarium has either a +II or +III oxidation state in sulfide compounds (5–8), one can expect in lillianite type structures, a SmCr$_2$S$_4$ formulation with Sm^{2+}, a Sm$_{2/3}$Cr$_2$S$_4$ formulation with Sm^{3+}, or an intermediate phase with mixed valence for samarium. This study shows that the present Sm derivative is stabilized with Sm^{3+}. In addition to a threefold commensurate superstructure along **a** (as found in Gd$_{2/3}$Cr$_2$S$_4$), an incommensurate superstructure along the **b** direction, close to $3 \times b$, occurs in Sm$_{2/3}$Cr$_2$S$_4$.

[1] To whom correspondence should be addressed.

EXPERIMENTAL

Synthesis. Sm$_{2/3}$Cr$_2$S$_4$ was obtained by sulfurization of a mixture of SmCrO$_3$ and Cr$_2$O$_3$ in a 1:1 ratio under a H$_2$S gas flow at 1300°C for 8 h. An unhomogeneous product was obtained. In a second step, single needle-like crystals with a metallic luster were formed in the low-temperature side (gradient of about 50°C between 950 and 1000°C) of a tube sealed under vacuum by using iodine as a transport agent.

Chemical analyses were performed at the BRGM-CNRS common laboratory (Orleans, France) using a Cameca SX-50 electron microprobe. Operating conditions were as follows: accelerating voltage 20 kV, beam current 15 nA, standards (element, X-ray emission line) FeS$_2$ (S$K\alpha$); (Sm, Nd, Yb, Lu, Al) complex oxide (Sm, Lα); Cr$_2$O$_3$ (Cr$K\alpha$). Analyses made on several crystals mounted in epoxy (polished section) obtained average contents (wt%): Sm, 34.4(1); Cr, 30.7(1); S, 38.6(1); total, 103.7(2). Even though the total weight content largely exceeds 100% (probably because of an inhomogeneous samarium standard), the Cr and S weight percentages agree quite well with the theoretical values calculated from the Sm$_{2/3}$Cr$_2$S$_4$ formulation (Cr, 31.28 and S, 38.58). Considering a SmCr$_2$S$_4$ chemical formulation, these theoretical contents would have been 27.18 and 33.52, respectively. A Sm$_{2/3}$Cr$_2$S$_4$ formulation leads to an exact charge balance between Sm^{3+}, Cr^{3+}, and S^{2-}.

Several trials were made to prepare homologous compounds with other lanthanide elements. They were not successful with lanthanum nor neodymium. The observation of polished sections of these preparations showed an intergrowth of chromium sulfide (Cr$_2$S$_3$) and the misfit layered compound ((LnS)$_{1+x}$CrS$_2$). This result proves that light lanthanide elements with accordingly too large Ln^{3+} ions cannot stabilize this kind of structure.

X-ray structural investigations. Weissenberg–Bragg studies revealed an orthorhombic symmetry with two superstructures ($=3 \times a$ and $\approx 3 \times b$). An X-ray powder

TABLE 1
X-Ray Powder Diffraction Pattern: Observed and Calculated Intensities for Main Reflections

h	k	l	d_{obs} (Å)	d_{calc} (Å)	I_{obs}	I_{calc}
2	0	2	4.153 (4)	4.1536	25	33
0	1	1	3.377 (2)	3.3788	16	25
1	1	1	3.2366 (11)	3.2278	6	9
0	0	4	3.1985 (11)	3.1997	32	32
3	0	2	3.1638 (11)	3.1640	58	73
1	0	4	3.0711 (10)	3.0706	11	11
1	1	2	2.957 (3)	2.9579	25	18
2	1	0	2.948 (2)	2.9484	8	14
0	1	3	2.707 (2)	2.7073	29	25
4	0	1	2.669 (2)	2.6699	22	18
1	1	3	2.6274 (3)	2.6278	100	100
4	0	2	2.5106 (6)	2.5110	37	35
1	0	5	2.492 (4)	2.4922	12	9
3	1	1	2.4764 (6)	2.4763	50	46
2	1	3	2.4247 (6)	2.4255	2	1
3	0	4	2.4028 (6)	2.4032	23	15
3	1	2	2.3479 (6)	2.3480	10	11
2	0	5	2.3158 (6)	2.3177	10	5
1	1	4	2.3085 (6)	2.3091	20	19
3	1	3	2.1702 (7)	2.1723	77	31
4	1	0	2.1531 (13)	2.1533	21	13
4	1	1	2.1234 (5)	2.1235	47	44
1	0	6	2.0931 (11)	2.0936	11	8
0	1	5	2.0670 (9)	2.0668	18	15
4	1	2	2.0412 (4)	2.0409	12	9
1	1	5	2.0306 (4)	2.0307	7	4
2	0	6	1.9869 (2)	1.9869	52	35
4	1	3	1.9220 (14)	1.9223	8	4
3	0	6	1.8409 (4)	1.8404	4	3
6	0	0	1.8197 (3)	1.8200	17	13
5	0	4	1.8032 (5)	1.8038	17	8
1	1	6	1.7975 (4)	1.7971	29	20
4	1	4	1.7867 (5)	1.7864	28	19
5	1	2	1.7802 (4)	1.7802	26	17
0	2	0	1.7515 (3)	1.7515	45	34
2	0	7	1.7341 (13)	1.7338	8	3
2	1	6	1.7283 (8)	1.7282	16	11
4	0	6	1.6809 (5)	1.6809	17	9
6	0	3	1.6740 (9)	1.6740	3	2
3	1	6	1.6295 (3)	1.6292	8	5
6	1	0	1.6144 (3)	1.6150	6	2
2	2	2	1.6144 (3)	1.6139	6	3
1	1	7	1.6027 (3)	1.6033	9	8
1	0	8	1.5827 (3)	1.5829	20	10
2	1	7	1.5542 (12)	1.5539	11	8
0	2	4	1.5362 (13)	1.5364	11	8
3	2	2	1.5327 (14)	1.5324	18	11
7	0	2	1.5157 (2)	1.5156	26	14
6	1	3	1.5107 (2)	1.5104	8	3
5	1	5	1.5016 (2)	1.5012	5	4
6	0	5	1.4835 (10)	1.4833	16	5
4	2	1	1.4649 (10)	1.4645	13	5
4	2	2	1.4368 (6)	1.4366	17	9
1	2	5	1.4333 (8)	1.4330	7	2
7	1	1	1.4183 (2)	1.4163	8	2
3	2	4	1.4160 (2)	1.4155	8	2
2	2	5	1.3971 (2)	1.3974	3	2
4	1	7	1.3940 (2)	1.3937	5	3
2	0	9	1.3764 (2)	1.3762	10	3
6	1	5	1.3661 (2)	1.3659	23	9
7	1	3	1.3519 (2)	1.3517	22	10
2	2	6	1.3143 (4)	1.3139	24	12
1	1	9	1.3084 (6)	1.3082	30	6
7	1	4	1.3018 (13)	1.3018	14	3
5	1	7	1.3018 (13)	1.3016	14	3
8	0	3	1.2999 (9)	1.3001	8	3
5	0	8	1.2907 (6)	1.2906	16	4
8	1	0	1.2717 (8)	1.2719	20	5
6	2	0	1.2622 (7)	1.2620	20	6

Note. Absorption effects are not taken into account in calculated intensities.

diffraction pattern was taken with a curved position sensitive detector (INEL apparatus) with strictly monochromatized $CuK\alpha_1$ radiation. Table 1 gives a list of observed and calculated intensities (9). Refinement of the unit-cell parameters of the basic structure (orthorhombic crystal

TABLE 2
(a) Crystallographic Data for $Sm_{2/3}Cr_2S_4$

Crystal data

Empirical formula	$Sm_{2/3}Cr_2S_4$
Formula weight	332.5 g/mol
Crystal dimensions	$0.45 \times 0.019 \times 0.042$ mm
Cell parameters (basic cell)	
a	3.5030 (3) Å
b	10.9199 (8) Å
c	12.7987 (8) Å
V	489.6 (1) Å^3
Modulation wave vectors	$\mathbf{q}_1 = \alpha_1\mathbf{a}^* + \alpha_2\mathbf{b}^*$ and
	$\mathbf{q}_2 = -\alpha_1\mathbf{a}^* + \alpha_2\mathbf{b}^*$
	$\alpha_1 = 0.3333(3); \alpha_2 = 0.3217(10)$
ρ_{calc}	4.51 g.cm^{-3}
ρ_{mes}	4.6 (3) g.cm^{-3}[a]
Z	4
μ	138 cm^{-1}

Data collection

Diffractometer	Enraf–Nonius CAD4
Radiation	$MoK\alpha$ ($\lambda = 0.71069$ Å)
θ range	$1.5° \leq \theta \leq 35°$
Indices range collection	
$h = p; p + 0.3333; p + 0.6667$	p: Integer $-5 \leq p \leq 5$
$k = p; p + 0.3217; p + 0.6783$	p: Integer $0 \leq p \leq 17$
l	$0 \leq I \leq 20$
Number of reflections recorded	2826
$l \leq 3\sigma(I)$	

(b) Crystallographic Data for $Sm_{2/3}Cr_2S_4$: Refinement Results

Basic structure refinement

Space group	*Pmnb*
Number of reflections	916
Number of refined parameters	43
Absorption correction	No
Type of refinement	Refinement based on F_{obs}
Reliability factors	
R^*	0.046
R_w^*	0.049
Highest positive peak in FD	$3.5.10^{-6}$ eÅ^{-3}
Highest negative peak in FD	$-2.8.10^{-6}$ eÅ^{-3}

Modulated structure refinement

	R^*	R_w^*
All reflections (1706)	0.063	0.083
Main reflections (916)	0.045	0.049
Satellites of order 1 (790)	0.104	0.124

Note. $*R = \Sigma(|F_{obs}| - |F_{calc}|/\Sigma(F_{obs})$; $R_w = (\Sigma w(|F_{obs}| - |F_{calc}|)^2/\Sigma w(F_{obs})^2)^{1/2}$; $w = 1/(\sigma^2(F_{obs}) + 0.02 \times F_{obs}^2)$.
[a] The measured density is imprecise because of the small amount of crystals available (25.1 mg).

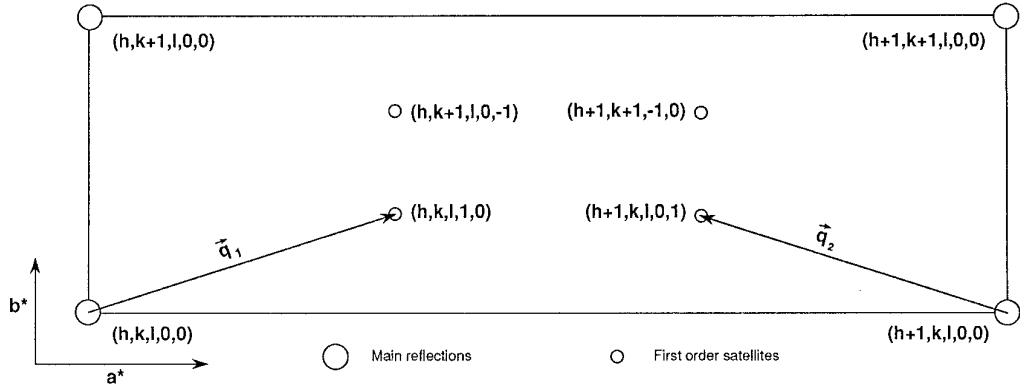**FIG. 1.** Reciprocal cell a^*, b^* of $Sm_{2/3}Cr_2S_4$ showing the two wave vectors needed to describe the modulated structure.

system) led to $a = 3.5030(3)$ Å, $b = 10.9199(8)$ Å, and $c = 12.7987(8)$ Å. This corresponds to a similar unit cell as reported for the $Gd_{2/3}Cr_2S_4$ compound.

X-ray films showed unusual reflection conditions. Any conventional space group, with a large cell $3a \times 3b \times c$, fits these conditions. All attempts of cell parameter refinement in this large cell lead to a triclinic deviation. These two features led us to consider the superstructure along **b** as an incommensurate one. In the basic reciprocal cell (a^*, b^*, c^*) all reflection spots may be indexed with five indices $hklmn$, $\mathbf{H} = h\mathbf{a}^* + k\mathbf{b}^* + l\mathbf{c}^* + m\mathbf{q}_1 + n\mathbf{q}_2$, using the two modulation vectors $\mathbf{q}_1 = \alpha_1\mathbf{a}^* + \alpha_2\mathbf{b}^*$ and $\mathbf{q}_2 = -\alpha_1\mathbf{a}^* + \alpha_2\mathbf{b}^*$ (see Fig. 1). The α_1 and α_2 parameters were refined with 89 reflections, collected from a single crystal, using the U-FIT program (10). The α_1 value converged to 0.3333 (3) while α_2 converged to 0.3217 (10). The collection was carried out on an Enraf–Nonius CAD4 diffractometer. Non-integer indices were used to record all reflections. Data collection conditions are given in Table 2. A total of 2826 reflections with $I \geq 3\sigma(I)$ were collected. Normal data corrections were carried out (decay and Lorentz polarization). No absorption correction was applied since all attempts to improve internal consistency of the data set using a correction based on the crystal shape ($0.45 \times 0.019 \times$ 0.042 mm) failed. Averaging according to the mmm Laue symmetry led to 916 main reflections and 790 first-order satellites with $I \geq 3\sigma(I)$ observation criterion. The JANA chain programs (11) were used for all these refinement calculations.

CRYSTALLOGRAPHY

Average structure refinement. The observed systematic absences in the main-reflection set ($h0l$, $h + l = 2n$; $hk0$, $k = 2n$; $00l$, $l = 2n$) are consistent with the centrosymmetric space group *Pmnb* (#62) and the noncentrosymmetric space group $P2_1nb$ (#33). The structure was solved by Patterson and Fourier difference methods in *Pmnb*. The site occupancy factor (s.o.f.) for the samarium atom was refined and converged to 0.3305(15). This occupancy agrees very well with the theoretical value of $\frac{1}{3}$ expected from the charge equilibrium and the chemical analysis result. Final refinements led to reliability factors $R = 0.046$ and $R_w = 0.049$. All structure parameters are given in Table 3. The main interatomic distances are listed in Table 4.

Modulated structure refinement. Due to the fact that two wave vectors are needed to index the whole diffraction

TABLE 3
Atomic Parameters of the Average Structure of $Sm_{2/3}Cr_2S_4$ (Space group *Pmnb*)

Atom	site	x	y	z	s.o.f.[a]	B_{eq} (Å^2)
Sm	8(d)	0.3002 (3)	0.23585 (6)	0.32994 (5)	0.3305 (15)	B_{iso} = 0.51 (2)
Cr1	4(c)	1/4	0.05431 (11)	0.11253 (10)	1	0.42 (2)
Cr2	4(c)	1/4	0.08486 (11)	0.59624 (9)	1	0.42 (2)
S1	4(c)	1/4	0.2997 (2)	0.65563 (15)	1	0.54 (3)
S2	4(c)	1/4	0.3816 (2)	−0.02917 (15)	1	0.52 (3)
S3	4(c)	1/4	0.0892 (2)	−0.07132 (14)	1	0.44 (3)
S4	4(c)	1/4	−0.0329 (2)	0.28582 (15)	1	0.65 (4)

^{a} Site occupancy factor (s.o.f.)

<div align="center">

TABLE 4
Main Interatomic Distances (Å) in the Average Structure of $Sm_{2/3}Cr_2S_4$

</div>

			a					a
Sm	Sm	3.8595 (15)	#1		Cr1	S1	2.4364 (17)	#3
	Sm	0.3515 (15)	#2		Cr1	S1	2.4364 (17)	#4
					Cr1	S3	2.3902 (18)	
	S1	2.9806 (21)	#3		Cr1	S3	2.4131 (16)	#9
	S1	2.7660 (22)	#4		Cr1	S3	2.4131 (16)	#11
	S2	2.9404 (15)	#5		Cr1	S4	2.4207 (19)	
	S2	2.7227 (16)	#6		⟨Cr1–S⟩		2.4183	
	S3	2.9996 (17)	#5					
	S3	2.7865 (18)	#6		Cr2	S1	2.4714 (25)	
	S4	3.0007 (23)			Cr2	S2	2.3857 (24)	#12
	S4	2.9401 (21)	#7		Cr2	S2	2.4091 (12)	#5
⟨Sm–S⟩		2.8921			Cr2	S2	2.4091 (12)	#6
					Cr2	S4	2.3861 (12)	#10
Cr1	Cr1	3.5080	#8		Cr2	S4	2.3861 (12)	#13
Cr1	Cr1	3.5821 (16)	#9		⟨Cr2–S⟩		2.4079	
Cr2	Cr2	3.5080	#8					
Cr2	Cr2	3.5547 (14)	#10					

Note. ESD given in parentheses; deviation on cell parameters is not taken into account.

[a] Symmetry transformations used to generate equivalent atoms: #1: $-\frac{1}{2} - x, y, z$; #2: $\frac{1}{2} - x, y, z$; #3: $-x, \frac{1}{2} - y, -\frac{1}{2} + z$; #4: $1 - x, \frac{1}{2} - y, -\frac{1}{2} + z$; #5: $-x, \frac{1}{2} - y, \frac{1}{2} + z$; #6: $1 - x, \frac{1}{2} - y, \frac{1}{2} + z$; #7: $x, \frac{1}{2} + y, \frac{1}{2} - z$; #8: $1 + x, y, z$; #9: $-x, -y, -z$; #10: $-x, -y, 1 - z$; #11: $1 - x, -y, -z$; #12: $x, -\frac{1}{2} + y, \frac{1}{2} - z$; #13: $1 - x, -y, 1 - z$.

<div align="center">

TABLE 5
Symmetry Operations of the (3 + 2)D Superspace Group $Pmnb(\alpha\beta0)g\dot{m}g$ Used to Describe the Modulated Structure of $Sm_{2/3}Cr_2S_4$

</div>

$$\{E, 1|n_1\ n_2\ n_3\ n_4\ n_5\} \qquad \{i, 2|0\ 0\ 0\ 0\ 0\}$$

$$\{2_x, \dot{m}|\tfrac{1}{2}\ 0\ 0\ \tfrac{1}{2}\ \tfrac{1}{2}\} \qquad \{2_y, \dot{m}|\tfrac{1}{2}\ \tfrac{1}{2}\ \tfrac{1}{2}\ 0\ 0\} \qquad \{2_z, 2|0\ \tfrac{1}{2}\ \tfrac{1}{2}\ \tfrac{1}{2}\ \tfrac{1}{2}\}$$

$$\{m_x, \dot{m}|\tfrac{1}{2}\ 0\ 0\ \tfrac{1}{2}\ \tfrac{1}{2}\} \qquad \{m_y, \dot{m}|\tfrac{1}{2}\ \tfrac{1}{2}\ \tfrac{1}{2}\ 0\ 0\} \qquad \{m_z, 1|0\ \tfrac{1}{2}\ \tfrac{1}{2}\ \tfrac{1}{2}\ \tfrac{1}{2}\}$$

$$E = \begin{pmatrix} 1 & 0 & 0 \\ 0 & 1 & 0 \\ 0 & 0 & 1 \end{pmatrix} \qquad i = \begin{pmatrix} -1 & 0 & 0 \\ 0 & -1 & 0 \\ 0 & 0 & -1 \end{pmatrix}$$

$$2_x = \begin{pmatrix} 1 & 0 & 0 \\ 0 & -1 & 0 \\ 0 & 0 & -1 \end{pmatrix} \quad 2_y = \begin{pmatrix} -1 & 0 & 0 \\ 0 & 1 & 0 \\ 0 & 0 & -1 \end{pmatrix} \quad 2_z = \begin{pmatrix} -1 & 0 & 0 \\ 0 & -1 & 0 \\ 0 & 0 & 1 \end{pmatrix}$$

$$m_x = \begin{pmatrix} -1 & 0 & 0 \\ 0 & 1 & 0 \\ 0 & 0 & 1 \end{pmatrix} \quad m_y = \begin{pmatrix} 1 & 0 & 0 \\ 0 & -1 & 0 \\ 0 & 0 & 1 \end{pmatrix} \quad m_z = \begin{pmatrix} 1 & 0 & 0 \\ 0 & 1 & 0 \\ 0 & 0 & -1 \end{pmatrix}$$

$$1 = \begin{pmatrix} 1 & 0 \\ 0 & 1 \end{pmatrix} \quad 2 = \begin{pmatrix} -1 & 0 \\ 0 & -1 \end{pmatrix} \quad \dot{m} = \begin{pmatrix} 0 & 1 \\ 1 & 0 \end{pmatrix} \quad \dot{m} = \begin{pmatrix} 0 & -1 \\ -1 & 0 \end{pmatrix}$$

Note. The (3 + 2)D symmetry operations are represented by $\{R_E, R_I|\nu_1\ \nu_2\ \nu_3\ \nu_4\ \nu_5\}$ where R_E and R_I are the symbols of the symmetry elements in external and internal space, respectively. $(\nu_1\ \nu_2\ \nu_3)$ and $(\nu_4\ \nu_5)$ are the associated fractional translation vectors in external and internal space, respectively.

pattern, a (3 + 2)D superspace group was used for the refinement of the complete structure. The superspace group is derived from the basic $Pmnb$ 3D-space group by considering the systematic absences in the $hklmn$ reflections set.

The (3 + 2)D Bravais class that is compatible with the external Bravais class and the two wave vectors is $Pmmm(\alpha\beta0)$ (12). The observed extinction condition $hk0mn$: $k + m + n = 2N$ leads to a nonprimitive origin-independent (3 + 2)D translation vector of $(0, \frac{1}{2}, 0, \frac{1}{2}, \frac{1}{2})$, associated with the b-glide plane. The symmetry operations used for the refinements are compiled in Table 5. The space group symbol tentatively constructed for this set of symmetry operations is $Pmnb(\alpha\beta0)g\dot{m}g$. Structure parameters are given in Tables 6a and 6b.

STRUCTURE DESCRIPTION

Figure 2 shows the projection of the average structure of $Sm_{2/3}Cr_2S_4$ onto the (b, c) plane. This structure is quite similar to that of $Gd_{2/3}Cr_2S_4$. Double columns of edge-sharing $[CrS_6]$ octahedra are found and samarium atoms are in bicapped trigonal prisms between these double columns. In Fig. 3, the $[CrS_6]$ octahedra are shown to form tunnels in which Sm atoms are statistically distributed with an s.o.f. of $\frac{1}{3}$.

Recently, Makovicky and co-workers have proposed a classification of all members of the lillianite family (3). In this formalism, $Sm_{2/3}Cr_2S_4$ can be denoted as a $^{2,2}L$ distorted structure type where the two superscript integers

TABLE 6

(a) Atomic Positions, Displacement Parameters of the Incommensurate Structure of $Sm_{2/3}Cr_2S_4$

Atom	x	y	z	s.o.f.	B_{eq} (Å^2)
Sm	0.311 (4)	0.2357 (6)	0.32922 (6)	0.33333	0.27 (4)
Cr1	1/4	0.0544 (2)	0.11253 (15)	1	0.30 (3)
Cr2	1/4	0.0849 (2)	0.59624 (14)	1	0.34 (3)
S1	1/4	0.2996 (3)	0.6557 (2)	1	0.44 (5)
S2	1/4	0.3815 (3)	−0.0292 (2)	1	0.42 (5)
S3	1/4	0.0892 (3)	−0.0713 (2)	1	0.38 (5)
S4	1/4	−0.0329 (3)	0.2858 (2)	1	0.46 (6)

(b) Modulation Parameters of Atomic Positions in the Incommensurate Structure of $Sm_{2/3}Cr_2S_4$

Sm	P_0	A_{10}	B_{10}	A_{01}	B_{01}	
	0.33333	0.368 (8)	0.12 (2)	0.376 (7)	−0.14 (2)	
	$A^x_{(10)}$	$A^y_{(10)}$	$A^z_{(10)}$	$B^x_{(10)}$	$B^y_{(10)}$	$B^z_{(10)}$
	−0.004 (3)	−0.0004 (5)	0.0034 (6)	−0.001 (4)	−0.0007 (5)	0.0023 (7)
	$A^x_{(01)}$	$A^y_{(01)}$	$A^z_{(01)}$	$B^x_{(01)}$	$B^y_{(01)}$	$B^z_{(01)}$
	−0.006 (3)	0.0009 (5)	−0.0022 (6)	0.012 (4)	−0.0006 (4)	0.0018 (6)
	$A^x_{(10)}$	$A^y_{(10)}$	$A^z_{(10)}$	$B^x_{(10)}$	$B^y_{(10)}$	$B^z_{(10)}$
Cr1[a]	0.0011 (9)	−0.0005 (3)	0.0020 (3)	0.0013 (8)	−0.0024 (3)	−0.0012 (3)
Cr2[a]	−0.0014 (9)	0.0006 (3)	0.0006 (3)	−0.0043 (9)	−0.0002 (3)	−0.0003 (3)
S1[a]	0.0002 (12)	−0.00007 (4)	−0.00008 (4)	−0.0000 (1)	0.0003 (4)	−0.0039 (4)
S2[a]	−0.0060 (14)	0.0001 (4)	0.0019 (4)	0.0015 (14)	0.00082 (4)	0.0021 (4)
S3[a]	0.0018 (13)	−0.0010 (4)	−0.0006 (4)	−0.0026 (14)	0.0015 (4)	−0.0005 (4)
S4[a]	0.0011 (14)	0.0001 (4)	−0.0003 (4)	0.0043 (14)	−0.0061 (4)	−0.00083 (4)

[a] These atoms are in special position 4(c) and thus the parameters of position modulation for the two waves along X_4 and X_5 are linked by the conditions $A^x_{(10)} = A^x_{(01)}; B^x_{(10)} = B^x_{(01)};$ $A^y_{(10)} = −A^y_{(01)}; B^y_{(10)} = −B^y_{(01)}; A^z_{(10)} = −A^z_{(01)}; B^z_{(10)} = −B^z_{(01)}.$ These parameters correspond to the formulae $X_i = X^\circ_i + A^i_{(10)} \sin(2\pi X_4) + B^i_{(10)} \cos(2\pi X_4) + A^i_{(01)} \sin(2\pi X_5) − B^i_{(01)} \cos(2\pi X_5). i = 1, 2, 3,$ corresponding to $x, y,$ or z.

are the numbers of edge-sharing octahedra which link two trigonal prisms, here two on both sides.

In the space group *Pmnb*, the general position $x\,y\,z$ of Sm atom leads to an equivalent position at $\frac{1}{2} − x\,y\,z$. With $x = 0.30$, these two positions are too close to be filled simultaneously. With an s.o.f. $\approx \frac{1}{3}$, one can assume an ordered distribution in relation with the $3 \times a$ superstructure. This hypothetical distribution is illustrated in Fig. 4. Thus, Sm–Sm distances (3.8595 Å) should be larger than the a value ($a = 3.5030$ Å) and close to those commonly reported. However, in the parent compound $Gd_{2/3}Cr_2S_4$, this model was not validated by the structural determination in a large unit cell (3a, b, c).

DISCUSSION

By comparing the two structural determinations (average and incommensurate), three features can be underlined:

• The shift between the $x\,y\,z$ and $\frac{1}{2} − x\,y\,z$ positions of Sm atoms is slightly larger in the modulated structure ($x_{modul} = 0.31$ and $x_{basic} = 0.30$).

• The occupancy modulation of the Sm atoms is quite important. The occupancy factor can be written as

$$P = 0.333333 + 0.368 \sin(2\pi X_4) + 0.12 \cos(2\pi X_4) \\ + 0.376 \sin(2\pi X_5) − 0.14 \cos(2\pi X_5). \quad [1]$$

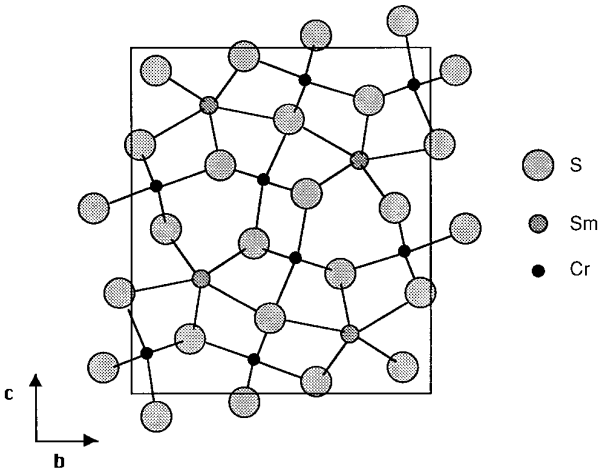This leads to large variations of the term $−0.455 \le P \le 1.122$. Values outside the 0–1 range are due to the fact

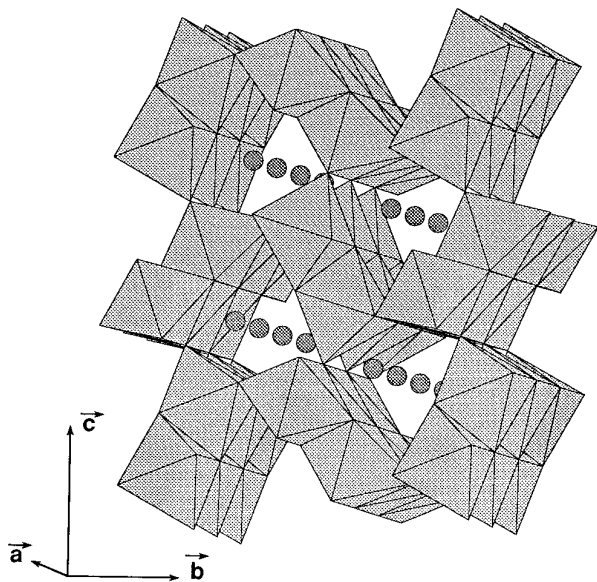**FIG. 2.** Projection on the (b, c) plane of the average structure of $Sm_{2/3}Cr_2S_4$.

FIG. 3. Perspective view of the average structure of $Sm_{2/3}Cr_2S_4$ showing the $[CrS_6]$ octahedra sequences.

that only one harmonic of the modulation function has been taken into account in the refinement.

• All the B_{eq} values are smaller in the case of the modulated structure than in the other case. This is a general result; in the basic structure, the atomic displacement parameter includes a part of the modulation on the atomic position.

The occupancy factor of samarium atoms was calculated from Eq. [1], using the LINE program (13) for a large
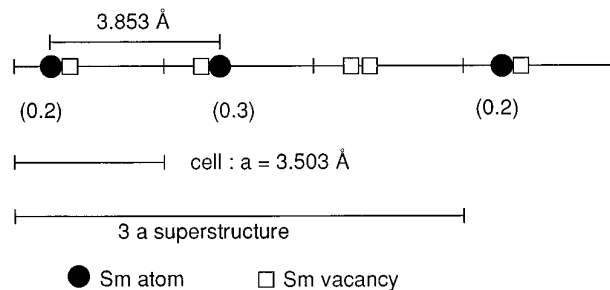
FIG. 4. Hypothetical model of the samarium distribution along the a direction.

number of unit cells in the (a, b) plane. Cells are numbered from an arbitrary origin and are labeled by (n_x, n_y). Figure 5 shows the occupation factor along the commensurate $\mathbf{a}$ direction for the Sm position $x = 0.31$ in rows $n_y = 0$, $n_y = 1$, and $n_y = 2$. The variation is periodic with a $3 \times a$ period, as expected. One can observe that there are no fully occupied positions for two successives sites in the $\mathbf{a}$ direction ($x = 0.31, x = 1.31, x = 2.31$, etc.). This samarium distribution is more complex than that described by the model drawn in Fig. 4. Nevertheless, the occupational modulation found by the modulated refinement is consistent with this simple model of domains alternating along $\mathbf{a}$.

The distribution of samarium atoms along $\mathbf{b}$ is very complex because of the incommensurate character of the structure along this direction. Figure 6 shows the samarium occupancy factor for the two equivalent positions $x = 0.19$ and $x = 0.31$, in the $n_x = 0$ row. The occupation curve tends toward a block-wave-type modulation, i.e., the occupation of a site is either 1 or 0. For a large number of sites, it is clear whether it is occupied or not, but for a certain
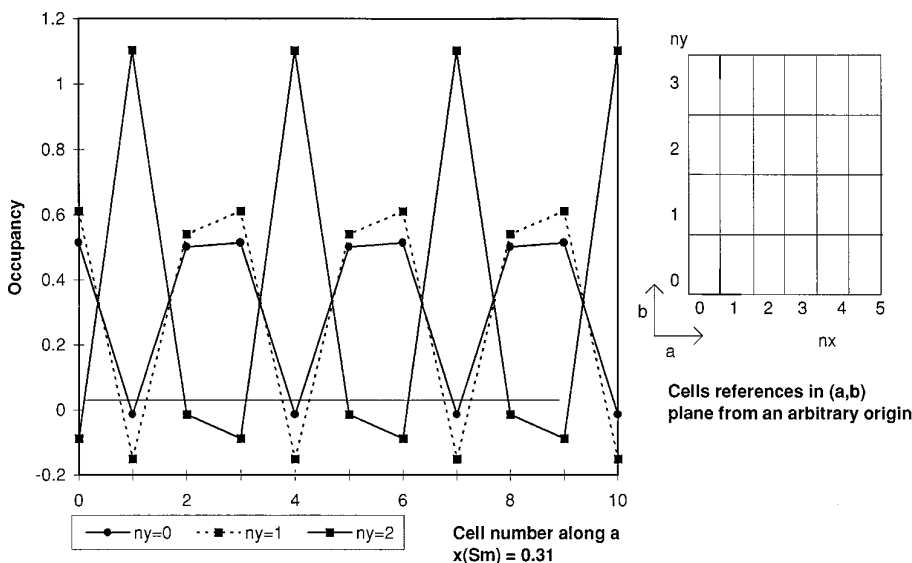

FIG. 5. Variation of the Sm occupancy factor for consecutive cells along $\mathbf{a}$.
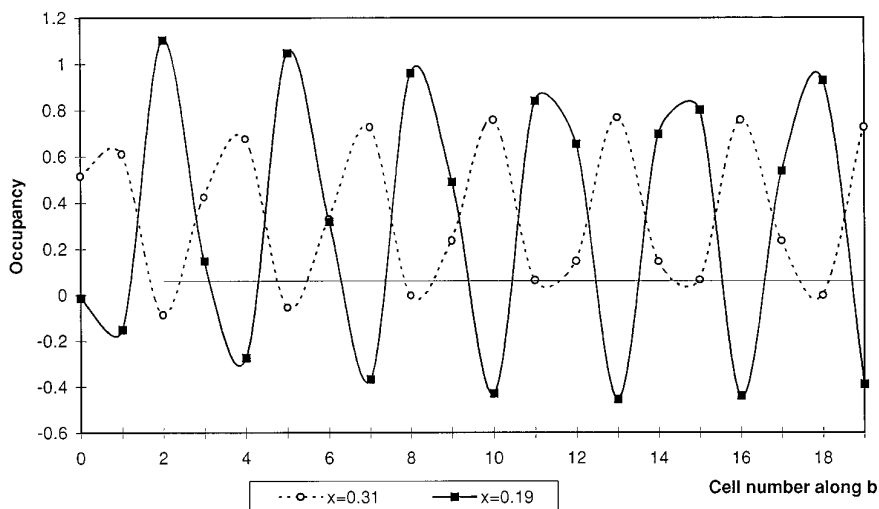
FIG. 6. Variation of Sm occupancy factor versus the cell number along **b** showing the incommensurate character of the modulation.

fraction of sites it is difficult to decide whether the occupation is 1, 0, or even fractional (statistical occupation). This makes it difficult to identify filled and unfilled domains along the incommensurate direction. It is plausible, however, that the incommensurate character of the modulation stems from an energetic competition between the in-cell $x = 0.19$ and $x = 0.31$ positions along **b**. In other words, the Sm ion "hesitates" between these two positions in an ordered way that is not compatible with the translational symmetry along this direction. This interpretation is supported by the fact that no modulation develops in the structure of $Gd_{2/3}Sm_2S_4$ where there is only one Gd position in each cell along the **b** direction. The difference between these two structures originates probably from the different ionic radii of Gd^{3+} and Sm^{3+} ($Sm^{3+} > Gd^{3+}$). The nonexistence of compounds of this structure type for larger lanthanide elements (La^{3+}, Nd^{3+}) proves that there is a limiting cation size for stabilizing this structure type. This limit lies near the ion radius of Sm^{3+}. The structure of $Sm_{2/3}Cr_2S_4$ is stable because of the incommensurability of the occupation of Sm^{3+} along **b**.

REFERENCES

1. T. Takahashi, K. Ametani, and O. Yamada, *J. Cryst. Growth* **24–25,** 151 (1974).
2. A. Meerschaut, A. Lafond, L. M. Hoistad, and J. Rouxel, *J. Solid State Chem.* **111,** 276 (1994).
3. E. Makovicky and S. Karup-Moller, *N. Jb. Miner. Abh.* **130**(3), 264 (1977).
4. E. Makovicky, *N. Jb. Miner. Abh.* **131**(2), 187 (1977).
5. O. Pena, Ph.D. thesis, University of Grenoble, France, 1979.
6. A. Jayaraman, E. Bucher, and R. G. Maines, *Phys. Rev. Lett.* **25,** 1430 (1970).
7. E. Bucher, V. Narayanamurti, and A. Jayaraman, *J. Appl. Phys.* **42,** 1741 (1971).
8. M. B. Maple and D. Wohlleben, *Phys. Rev. Lett.* **27,** 511 (1971).
9. W. Kraus and G. Nolze, *J. Appl. Cryst.* **29,** 301 (1996).
10. M. Evain, "U-FIT: A Cell Parameter Refinement Program." Institut des Matériaux de Nantes, France, 1992.
11. V. Petricek, "JANA 94 Programs for Modulated and Composite Crystals," Institute of Physics, Praha, Czech Republic.
12. A. Janner, T. Janssen, and P. M. de Wolff, *Acta Crystallogr. Sect. A* **39,** 671 (1983).
13. A. van der Lee, Institut des Matériaux de Nantes, France, 1993.